Some results of laboratory experiments on batch centrifugal ball milling

by D. I. HOYER*, B.Sc. (Chem. Eng.), M.I.Ch.E., and M. F. DAWSON*, Pr. Eng., M.Sc., M.S.A.I.M.M.

SYNOPSIS

The results obtained from the operation of a batch centrifugal ball mill are reported, together with the development of a model for the behaviour of a particle in free flight within the mill, and the introduction of a cumulative breakage rate function. Schumann and Rosin–Rammler plots show the change in particle-size distribution with time at various configurations of the mill. Graphs showing the rate of production of fines and the rate of breakage of coarse particles are included.

SAMEVATTING

Die resultate wat verkry is deur die bedryf van 'n sentrifugale lotbalmeul word beskryf tesame met die ontwikkeling van 'n model van die gedrag van 'n partikel in vrye vlug in die meul en die voorstelling van 'n funksie wat die breektempo aangee. Schumann- en Rosin–Rammler-grafieke toon die verandering in die partikel-grootteverdeling met tyd vir verskillende meulkonfigurasies. Daar word ook grafieke ingesluit wat die produksietempo van fynstof en die breektempo van growwe partikels toon.

INTRODUCTION

In a conventional cylindrical mill, a ball charge is tumbled under gravity, comminution taking place by grinding of the particles between the balls. The centrifugal ball mill operates within a centrifugal acceleration field, which is much stronger than that achieved under gravity. As a result, the rate of comminution is much higher.

The Chamber of Mines of South Africa Research Organization[1,2] investigated the potential value of the centrifugal mill to the South African mining industry, and showed that, because of the lower capital costs involved in the installation of the smaller machines required, centrifugal milling is more economically attractive than conventional milling.

Work on batch centrifugal ball milling was started at the University of Natal in 1979. The objects of the investigation were to obtain a better understanding of the crushing action in the centrifugal mill so that it would ultimately be possible for a comprehensive model of the behaviour of the mill under varying operating conditions to be formulated.

This paper presents some preliminary experimental results, and proposes a method for the modelling of these results using the cumulative breakage rate function. The results are presented as the rate of production of fines, the rate of disappearance of the coarse fractions, and the change, with grinding time, of particle-size distributions on Schumann and Rosin–Rammler curves.

NOMENCLATURE

a	Acceleration vector
a	Acceleration
C	Schumann size parameter, μm
d	Rosin–Rammler distribution coefficient
D	Mill diameter
g	Gravitational acceleration
G	Gyration diameter of mill about central axis
$G/2$	Gyration radius, i.e., the distance between the central axis and the mill axis
k	Cumulative breakage-rate parameter (Charles's Law constant)
L	Mill length
m	Schumann distribution coefficient
n	Cumulative breakage-rate parameter
N	Speed of rotation of the mill round the central axis, rad/s
N_c	Critical speed of mill
p	Position of particle in space (Cartesian co-ordinates)
P	Power, a particle, cumulative distribution
$Q(x)$	Mass fraction of material finer than sieve size
r	Radius
R	Gear ratio between mill and rotating arm of centrifugal mill
R_c	Critical gear ratio
t	Time
v	Velocity
v	Velocity vector
w	Mass fraction of material in a particular size x interval
W	Mass fraction of material larger than a certain particle size
x	Sieve size (μm) or space co-ordinate
x_0	Size of sieve through which 63,21 per cent of the material passes
Y	Space co-ordinate

THE CENTRIFUGAL MILL

As already mentioned, the centrifugal mill operates under a centrifugal acceleration field. One way for the centrifugal mill to be regarded is as a cylinder mounted at the end of an arm that rotates about a central axis. This is diagrammatically represented in Fig. 1. It should be noted that the mill rotates at $N.R$ rad/s relative to the rotating arm or at $N(R+1)$ rad/s relative to the earth.

The mechanics within the mill can be regarded as being either an acceleration field of constant direction observed from a rotating frame of reference, or a rotating

* Mintek Chemical Engineering Research Group, University of Natal, King George V Avenue, Durban 4001.

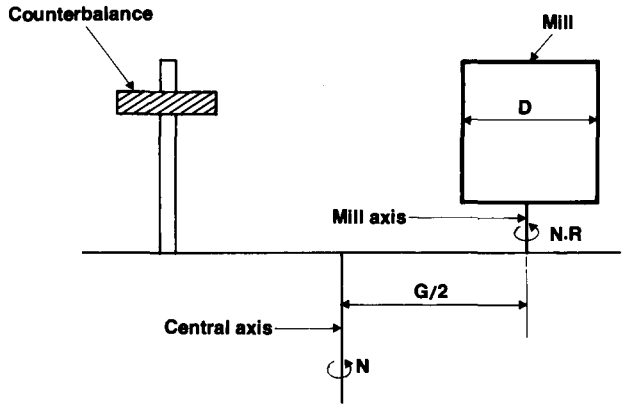

Fig. 1—Diagrammatic representation of the centrifugal mill

acceleration field observed from an inertial frame of reference.

From the first of these points of view, the mill rotates at a speed of $N.R$ in an acceleration field that varies in magnitude according to $a = N^2.r$, r being the distance from the central axis. Hence, r varies from $(G-D)/2$ to $(G+D)/2$ across the mill, and the magnitude of the acceleration vector varies from $a = N^2\ (G-D)/2$ at the point on the mill closest to the central axis to $a = N^2\ (G+D)/2$ at the point furthest from the central axis.

This variation in the acceleration field makes it necessary for the Coriolis effects on acceleration to be taken into account in the calculation of the trajectory of a particle. An observer on the axis of the mill would be in a rotating frame of reference, and Joisel[3] has shown that the path followed by a particle in free flight in the mill is a cycloid relative to the axis of the mill when the effect of gravity is assumed to be negligible.

The second way for the mechanics of the mill to be visualized is as follows. The mill rotates at a speed of $N(R+1)$ relative to the earth, and is acted upon by an acceleration field rotating at speed N. The magnitude of the acceleration vector is constant at $a = N^2.G/2$ (again on the assumption that gravitational acceleration is negligible). The validity of this view can be justified as follows. If the mill has a gear ratio of $R = -1$, it does not rotate relative to the earth, although every point on or in the mill gyrates at speed N at distance $G/2$ from a central point. Fig. 2 demonstrates that, if the mill rotates about point 0 at N rad/s, point P on the mill will rotate about 0′ at the same radius and speed. Similarly, all the other points on or in the mill rotate at speed N at radius $G/2$ round some point near 0. The direction of the acceleration of point P is given by the vector 0′P. From Fig. 2 it can be seen that this vector will always be equal to vector OC. Hence, the acceleration of every point P in or on the mill will be the same at any given moment, the magnitude being given by $a = N^2.G/2$ and the rotational speed by N rad/s. These conditions are identical to those that would arise if the mill were stationary and acted upon by a rotating acceleration field of constant magnitude. For gear ratios other than $R = -1$, the rotation of the mill at $N(R+1)$ rad/s must be taken into account. There is no Coriolis effect on acceleration, since the magnitude of the acceleration field is constant.

The motion of a particle P in free flight can be calculated if it is assumed that the particle leaves the wall at time $t = 0$, and that the direction of the acceleration field at $t = 0$ is that shown in Fig. 3 (i.e. 0 rad). The direction at time t will be $N.t$ rad and the acceleration vector will therefore vary with time as follows:

$$\text{a (o)} = [N^2\ (G/2),\ 0]$$

$$\text{a (t)} = [N^2\ (G/2)\cos N.t,\ N^2\ (G/2)\sin N.t].$$

Having ridden on the wall of the mill for some time, particle P will have the velocity of the corresponding point on the mill wall. If P leaves the mill wall at the point (x, y), its velocity vector at $t = 0$ is given by

$$\text{v (0)} = [-N(R+1)y,\ N(R+1)x].$$

The velocity at time t after P has left the mill wall is therefore given by

$$\text{v(t)} = \int_0^t \text{a}(t)\ \text{d}t$$

$$= [N(G/2)\sin N.t - N(R+1)y,\ -N(G/2)\cos N.t + N(G/2) + N(R+1)x].$$

In the calculation of the trajectory vector p(t) of P,

$$\text{p(0)} = [x,\ y]$$

and

$$\text{p(t)} = \int_0^t \text{v(t)}\ \text{d}t$$

$$= [-(G/2)\cos N.t - N(R+1)y.t + G/2 + x,\ -(G/2)\sin N.t + N(G/2)t + N(R+1)x.t + y],$$

i.e., the particle moves round the perimeter of a circle of diameter G at N rad/s, and the centre of the circle at a constant velocity.

This is the equation of a cycloid, and reinforces Joisel's argument[3]. The particle P will follow this trajectory until it again makes contact with the mill wall.

The mechanics governing the particles in a centrifugal mill are therefore not the same as those governing the particles in a gravitational mill, where a particle in free flight follows a parabolic trajectory. The difference is significant, as is shown by the following analysis of critical and non-critical conditions in the mill.

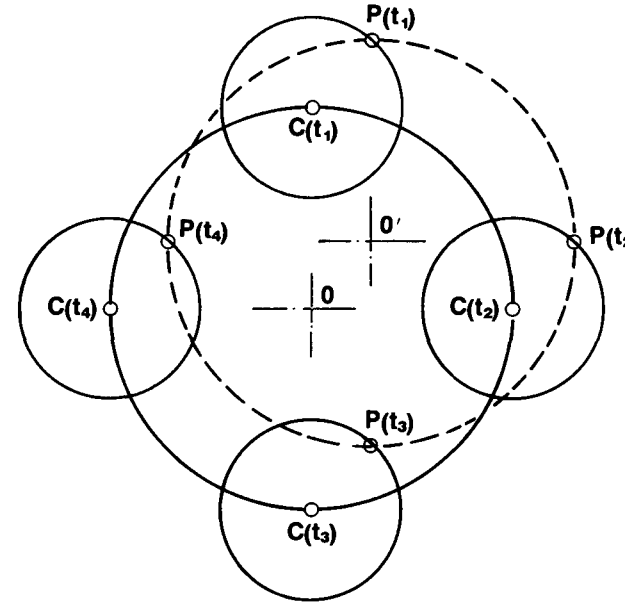

Fig. 2—Diagram to illustrate that, at $R = -1$, each point on or in the mill travels in a circular path about some centre O′ where the vector OO′ is equal to the vector CP

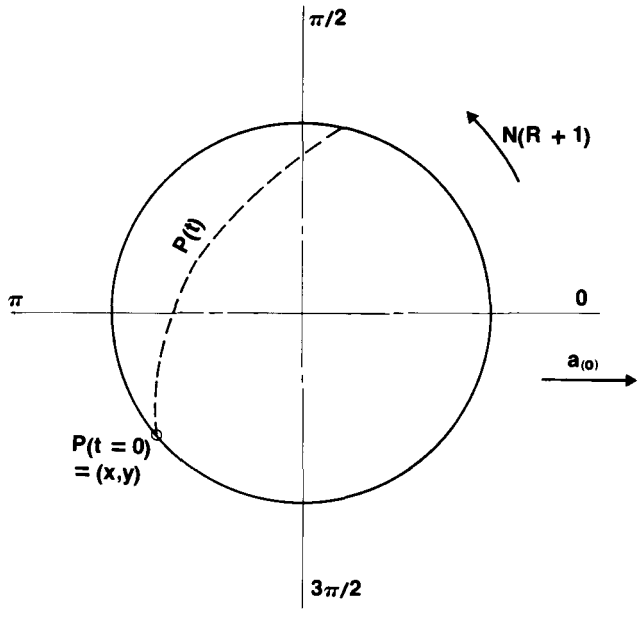

Fig. 3—The trajectory followed by a particle (P) leaving the mill wall is cycloidal relative to the axis of the mill

In a gravitational mill, the ball charge will ride round the mill wall when the centrifugal acceleration due to the rotation of the mill is greater than the gravitational acceleration. When this happens, the mill is said to 'go critical'. The minimum speed at which this occurs is called the critical speed, and is given by

$$N_c = \pm\sqrt{g/r}.$$

Bradley[1] has shown that, for the centrifugal mill, critical operation is determined by the gear ratio R rather than by the speed, and that the critical gear ratio is given by

$$R_c = -1 \pm\sqrt{G/D}.$$

This is significant because, at a gear ratio of $R = -1$, the mill can be operated at any G/D configuration without going critical and, secondly, if the mill is in a subcritical configuration, it can be operated at any speed. Hence, the power that can be put into a centrifugal mill is limited only by the mechanical strength of the mill and not by its size, as it is in a gravitational mill.

Bradley also proposed the following relation for power consumption (P):

$$P \propto D^3.L.R.G.N^3.$$

A small increase in speed results in a large increase in the power consumption (and hence a corresponding increase in the comminution rate). As a result, a small strongly constructed centrifugal mill can be made to achieve the same crushing rate as a much larger gravitational mill.

EXPERIMENTAL PROCEDURE

The mill used at the University of Natal was designed for operation at a wide range of configurations. The specifications for the mill are as follows:

mill size	150 mm in diameter by 150 mm in length
lifter bars	4 by 3 mm in height
R-ratio	variable from −2,7 to +2,7
G/D ratio	variable from 0,4 to 3,2
speed	variable from 100 to 700 r/min.

The mill is driven by a 55 kW motor via a set of chains. This method allows easy and accurate control over the speed and the gear ratio.

The mill charge in all the experimental runs carried out was 1 kg of quartz (put through a jaw crusher and sieved to material smaller than 6300 μm) and 2 kg of steel balls. All the runs were conducted at a gear ratio of $R = -1$, although the effect of variation in the gear ratio will be investigated in the near future. Three values were considered for G/D (0,4, 1,2, and 2,0), five for speed (303, 400, 487, 607, and 695 r/min), and six for ball size (5 mm, 7,5 mm, 10 mm, 15 mm, 20 mm, and 30 mm). At each configuration of the mill, three runs were carried out at different grinding times so that the change in size distribution with time could be observed.

After each run the sample was split on a riffler three times to approximately 125 g, weighed, wet-sieved through a 38 μm screen, and oven-dried to give the quantity of fines (material smaller than 38 μm) by difference. The remainder of the sample was then sieved through a $\sqrt{2}$-series of sieves from 4700 to 38 μm to give the complete size distribution.

The distributions obtained were then used in an attempt to determine trends that would be useful in the formulation of a model to describe breakage in the mill under varying operating conditions. The data include the rate of production of fines, the rate of disappearance of coarse particles, and the particle-size distributions plotted on Schumann and Rosin–Rammler curves. A more sophisticated technique examined was the calculation of a cumulative breakage rate function.

EXPERIMENTAL RESULTS

Schumann Distributions

Schumann noted that the plotting on log–log scales of cumulative size distributions obtained with different grinding times for the same feed sample often resulted in a series of parallel straight lines for an appreciable portion of the distributions. The equation of the straight-line region (i.e., the Schumann equation) is

$$Q(x) = C.x^m \qquad 0 \leqq Q(x) \leqq 1,$$

where m is the gradient of the curve when plotted as $\ln Q(x)$ versus $\ln x$ and is called the distribution coefficient, and C is the size at which $Q(x) = 1$ (extrapolated if necessary from the straight-line region of the experimental data).

The experimental results for a large number of runs under varying operating conditions were plotted on log–log scales. The curves obtained varied from reasonably straight lines for the finer sizes, flattening out near $Q(x) = 1$, to distinctly S-shaped curves with a central flat portion. Fig. 4 gives an example of a set of results that could be made to fit the Schumann equation fairly successfully, and Fig. 5 gives an example of the S-shaped curves, which obviously could not be made to fit the Schumann equation. The only difference in the operating conditions between these two sets of results is that 20 mm balls were used in the runs represented in Fig. 4, and 10 mm balls in the runs for Fig. 5. (The mill configuration

used was $G/D = 0{,}4$ and $R = -1$, at a speed of 607 r/min.). The explanation for the S-shaped curve is that the balls used were too small to break the quartz particles in the larger size fractions. Graphs in which the curves were straight could be obtained if the ball size or speed were increased. (An increase in speed would increase the centrifugal acceleration of the mill, which would cause the balls to strike with greater force.)

Charles proposed that C varies with grinding time according to the expression

$$k(t_2 - t_1) = \frac{1}{C_2{}^{m}} - \frac{1}{C_1{}^{m}},$$

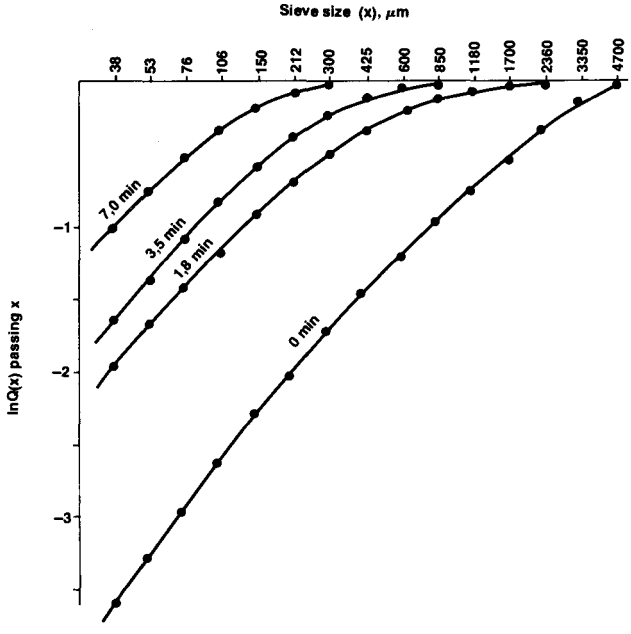

Fig. 4—Schumann distributions at a mill speed of 607 r/min with $R = -1$, $G/D = 0{,}4$, and balls of 20 mm diameter

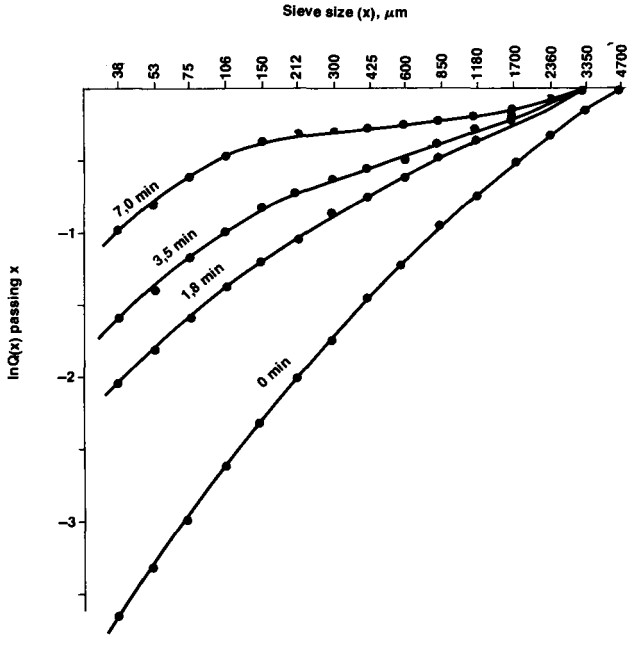

Fig. 5—Schumann distributions under the same conditions as for Fig. 4, except for ball size, which was reduced to 10 mm

where k is a constant.

The curves depicted in Fig. 4 were used in a test of the validity of Charles's Law for the experimental data. The graphs curve gently throughout the particle-size range, but can be approximated over the smaller sizes by straight parallel lines. Fig. 6 shows the position of the straight lines inserted for the same data as those depicted in Fig. 4. A value of 0,7 was obtained for m, and the values for C given in Table I were obtained by extrapolation of the straight lines to $\ln Q(x) = 0$ for each of the three grinding times. Values for k are given in Table II, being calculated from

$$k = \left(\frac{1}{t_2 - t_1}\right) \times \left(\frac{1}{C_2{}^{0,7}} - \frac{1}{C_1{}^{0,7}}\right).$$

The values obtained for k are reasonably consistent in view of the difficulty in the determination of accurate values for m and C.

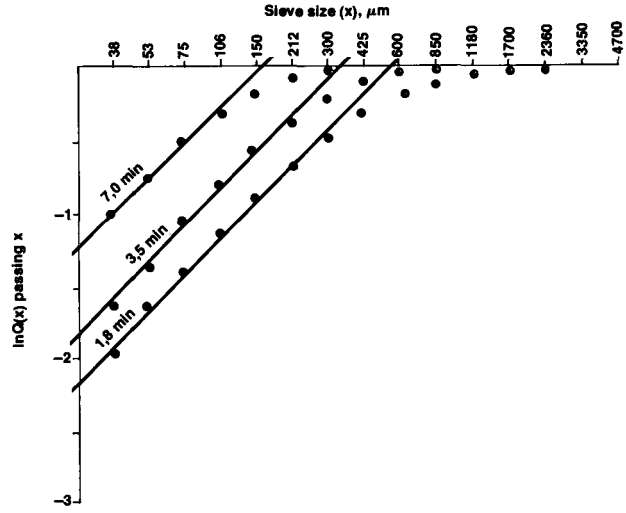

Fig. 6—Graphical determination, from the Schumann distributions, of the constants according to Charles's Law

TABLE I

VALUES FOR C OBTAINED FROM EXTRAPOLATION TO $Q(x) = 1$ OF THE STRAIGHT-LINE PORTIONS OF THE CURVES DEPICTED IN FIG. 6

Run no.	Grinding time min	C μm
1	1,8	550
2	3,5	350
3	7,0	160

TABLE II

VALUES FOR k OBTAINED FROM CHARLES'S LAW WITH THE VALUES FOR C SHOWN IN TABLE I AND WITH $m = 0{,}7$

Run no.	k $\times 10^{-3}$
1 to 2	2,57
1 to 3	3,16
2 to 3	3,45

Rosin–Rammler Distributions

Another model used fairly often in the representation of size distributions is the Rosin–Rammler equation, given by

$$Q(x) = 1 - \exp\left[-\left(\frac{x}{x_0}\right)^d\right],$$

where x_0 is the size of sieve through which 63,21 per cent of the material passes, and is a function of the grinding time. It has been found that the cumulative distributions obtained with a number of grinding times from the same feed sample will often yield a series of parallel straight lines in the plotting of

$$\ln \ln \frac{1}{1 - Q(x)} \text{ versus } \ln x,$$

indicating that d is a constant.

Like the Schumann plots, the Rosin–Rammler plots give reasonably straight lines in some circumstances and S-shaped curves in others. Figs. 7 and 8 demonstrate examples of good and bad Rosin–Rammler fits. Both sets of results were obtained at 607 r/min, $G/D = 1{,}2$, and R = −1, the difference being that 20 mm balls were used for one set of runs (Fig. 7) and 10 mm balls for the other (Fig. 8). S-shaped curves were again obtained when the balls were too small or the speed too low.

It is doubtful whether a commercial mill would be run under the conditions given in Figs. 5 and 8. Provided that the balls used are big enough to break the large particles, it seems that the Schumann and the Rosin–Rammler equations both provide a reasonable representation of the size distributions.

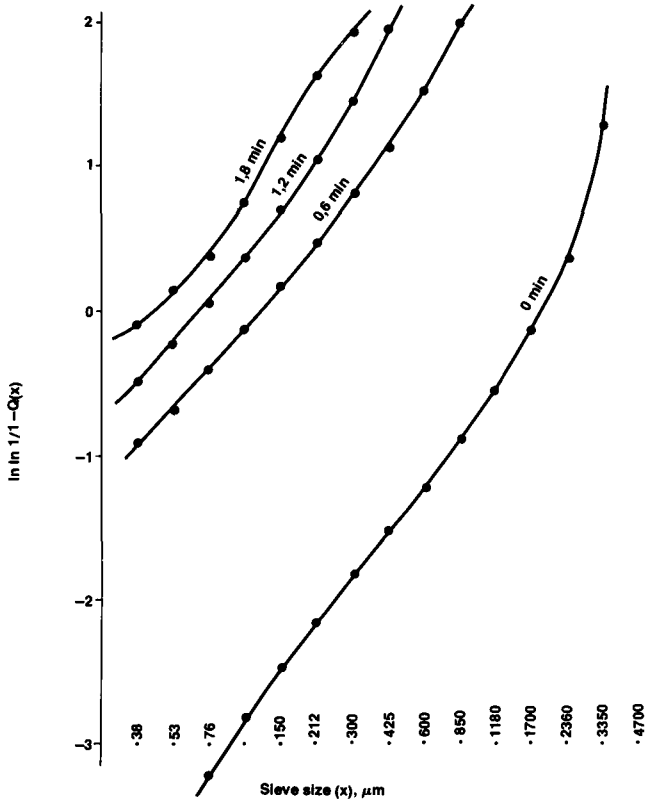

Fig. 7—Rosin–Rammler curves at 607 r/min, $G/D = 1{,}2$, and $R = -1$, 20 mm balls being used

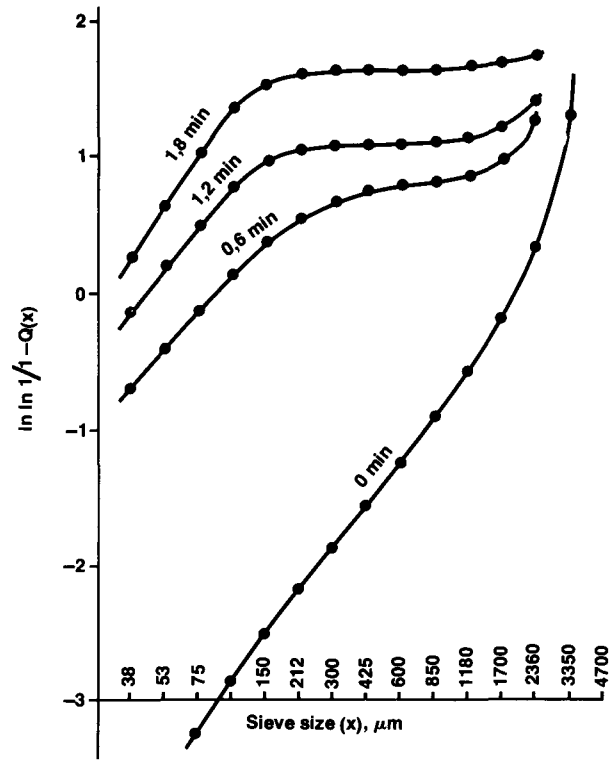

Fig. 8—Rosin–Rammler curves at 607 r/min, $G/D = 1{,}2$, and $R = -1$, 10 mm balls being used

Rate of Production of Fines

In milling it is often found that the production of fines has zero-order kinetics during the initial stages of grinding, i.e.,

$$\frac{dQ(x, t)}{dt} \text{ is constant for values of } Q(x, t) < 0{,}7.$$

In this investigation this was the case for the results obtained from the centrifugal mill.

The Effect of Ball Size

Fig. 9 shows the effect of ball size on the rate of production of material smaller than 38 μm with the mill running at 303 r/min, a gear ratio of $R = -1$, and a G/D value of 1,2. It can be clearly seen that the rate of production of fines increases with decreasing ball size. This is because the smaller the balls, the greater the number of balls in the mill and, hence, the greater the number of collisions per unit of time. Provided that the balls are sufficiently large to break the smaller particles, the rate of breakage will then depend on the number of balls rather than on the ball size. The graphs for the 15 and 20 mm balls show that the rate of production of the fines is initially rapid before settling down to a constant rate. This could be caused by some soft or pre-fractured quartz that breaks very quickly during the initial stages of milling.

The Effect of Mill Speed

The effect of speed on the production of fines was

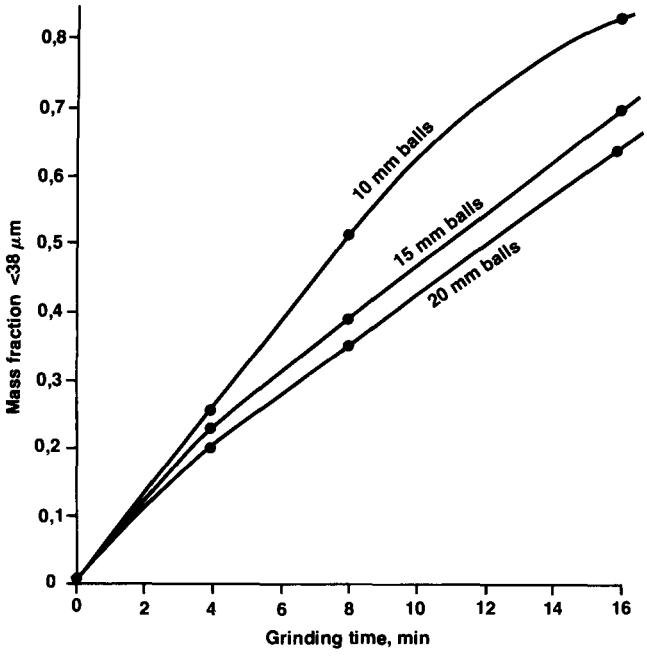

Fig. 9—The effect of ball size on the rate of production of fines at 303 r/min, $G/D = 1{,}2$, and $R = -1$

investigated, runs being carried out with 20 mm balls, a gear ratio of −1, and a G/D value of 1,2. The results, which are shown in Fig. 10, show that, as expected, the kinetics are zero order and that the rate of production increases with increasing speed. All these runs show a rapid initial production of fines before the mill settles down to a constant rate of production. The nature of the relation between the rate of production of fines and the speed of the mill was examined. The results are illustrated in Fig. 11, which shows that this relation appears to follow some simple power law. A least-squares regression showed that the rate of production of fines is proportional to $N^{2,6}$.

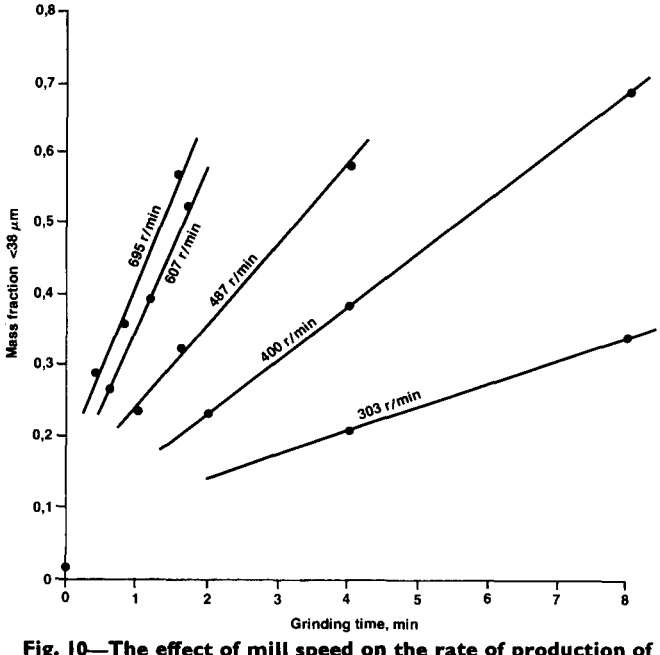

Fig. 10—The effect of mill speed on the rate of production of fines at $G/D = 1{,}2$ and $R = -1$, 20 mm balls being used

As mentioned earlier, it has been shown[1,2] that mill power is proportional to N^3. One could therefore conclude that the rate of production of fines is constant for values of $Q(x)$ up to about 0,7, and is approximately proportional to the power consumption. The constant of proportionality would be a function of the ball size.

Rate of Breakage of Coarse Particles

Another commonly found feature in milling is the first-order breakage of coarse particles, i.e.

$$\frac{dW}{dt} = -kW,$$

where W is the coarse fraction. The solution to this equation is

$$W(t) = W(0).\exp(-k.t),$$

where $W(0)$ is the coarse fraction at $t = 0$. In a first-order process, a plot of the mass fraction larger than a certain size (say, 1700 μm) on a log scale versus time on a linear scale yields a straight line of slope $-k$.

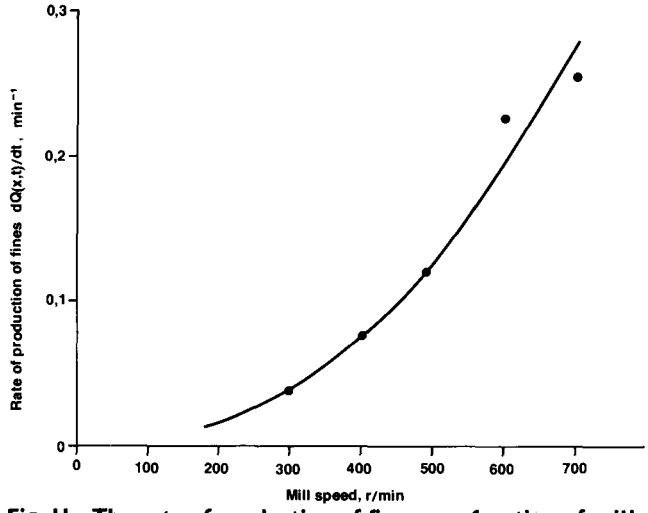

Fig. 11—The rate of production of fines as a function of mill speed, obtained by plotting the gradients of the graphs in Fig. 10 against the relevant speed

The Effect of Mill Speed

Fig. 12 is a plot of the disappearance of coarse material with time for various mill speeds. A departure from first-order kinetics is observed. (The operating conditions for these runs were $G/D = 1{,}2$ and $R = -1$, 10 mm balls being used.) As expected, the rate of breakage was much higher at higher speeds since the increased agitation results in more collisions. Also, the balls collide with greater force, resulting in a higher probability of breakage. The fact that the rate of breakage is not first order is clearly shown in Fig. 12, from which it can be seen that the rate is initially high, but that it then decreases slightly and finally increases again. The fast initial rate of breakage probably occurs for the same reason as does the fast initial production of fines, viz that some of the material is soft or pre-fractured, and breaks more readily than the rest. The curve would therefore be expected to have a steep gradient initially, becoming less steep with time until it approaches a straight line. As can be seen from Fig. 12, this does happen for a short time, but the gradient of the curve then becomes steeper again, and this effect cannot be as easily explained.

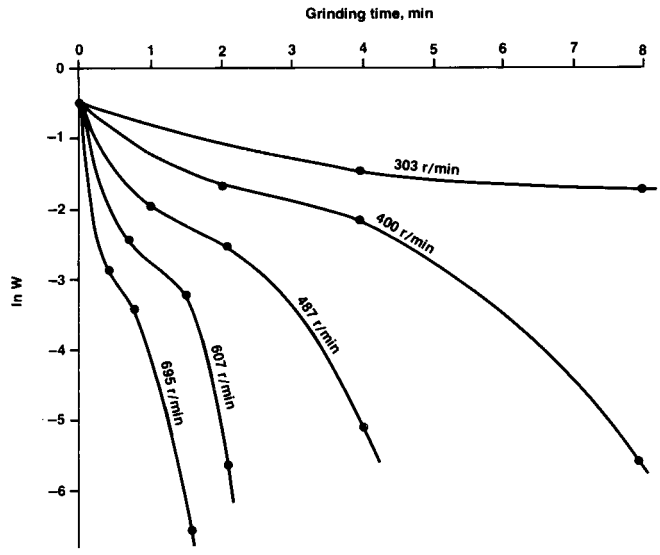

Fig. 12—The effect of mill speed on the disappearance of coarse particles (larger than 1700 μm) at $G/D = 1,2$ and $R = -1$, 10 mm balls being used

From the experimental data collected it has not yet been possible to determine the cause of this behaviour, although several possible explanations have been proposed[4] including the following.

(a) Within a given size interval, the larger particles shield the smaller particles from impact, which results in an overall increase in the rate of breakage within that size interval once the larger particles have been broken.

(b) The material might become progressively weaker with time owing to repeated impacts that weaken, but do not break, the larger particles.

(c) The efficiency of the crushing action might increase with an increase in the fraction of fines in the mill.

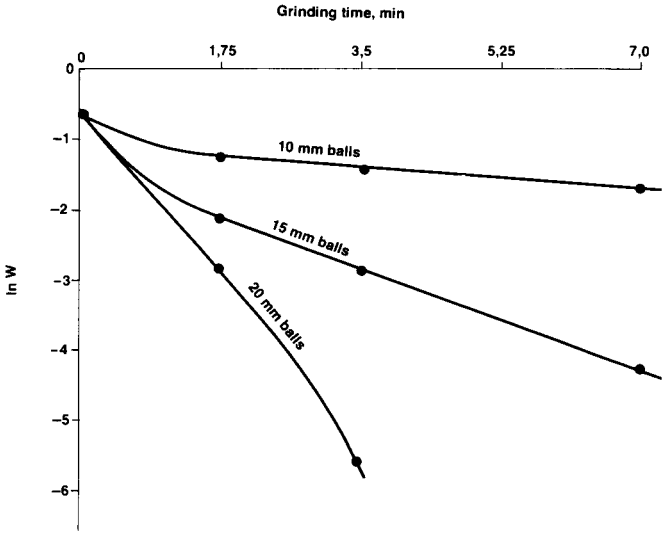

Fig. 13—The effect of ball size on the breakage rate of coarse particles (larger than 1700 μm) at 607 r/min, $R = -1$, and $G/D = 0,4$

The Effect of Ball Size

In an assessment of the effect of different ball sizes on the breakage rate of coarse fractions, three runs were carried out at 607 r/min, $R = -1$, and $G/D = 0,4$ with balls of 10 mm, 15 mm, and 20 mm diameter respectively. The results, which are illustrated in Fig. 13, show clearly that the rate of disappearance of material larger than 1700 μm is higher with increasing ball size. This is probably because a coarser particle needs repeated impacts by small (10 mm) balls to reduce it to less than 1700 μm, whereas a single impact by a large (20 mm) ball should suffice.

Cumulative Breakage Rate

It was decided that the rate of breakage of material larger than each size should be investigated as a possible way of modelling the behaviour of the mill. As mentioned earlier, the rate of breakage of the coarse fractions is often first order. However, with decreasing size, there is a marked departure from first-order kinetics, and it was proposed that n-th order kinetics should be assumed in the assessment of the data, i.e.

$$\frac{dW_i}{dt} = -k_i . W_i^{n_i}$$

for each size i, where

W_i is the cumulative fraction greater than size i, and k_i and n_i are parameters to be determined for each size i.

The solution to this equation is as follows:

$$W_i(t) = \left[W_i(0)^{(1-n_i)} - k_i t(1-n_i)\right]^{1/(1-n_i)}$$

$$\begin{cases} n \neq 1. \\ t \leqq W_i(0)^{(1-n_i)}/k_i(1-n_i) \end{cases}$$

and $W_i(t) = W_i(0) \exp(-k_i t)$ $\quad \{n = 1.$

For the general case of $n \neq 1$, $W_i(t)$ is zero for

$t = W_i(0)^{(1-n_i)}/k_i(1-n_i)$, and must obviously remain zero for larger values of t, when the above equation has no real solution.

For a graphical determination of the parameters k_i and n_i, the fraction of material larger than size x was plotted versus time for each size x, giving a series of graphs depicting $W_i(t)$ versus t. A typical example of such a plot is shown in Fig. 14. This particular case was for size 10 ($x = 212$ μm), with the mill operating at 303 r/min, $R = -1$, and $G/D = 1,2$. The size of the balls used was 20 mm. On each graph the gradient was measured for several values of $W_i(t)$, so that a table of values of $W_i(t)$ and corresponding values of $\frac{dW_i(t)}{dt}$ could be constructed. From these values a second series of graphs were plotted, showing $\ln\left(\frac{-dW_i(t)}{dt}\right)$ versus $\ln W_i(t)$. If the data follow the functional form given above, the graphs will be straight lines having the gradients equal to n_i, and the y-intercepts equal to $\ln(k_i)$.

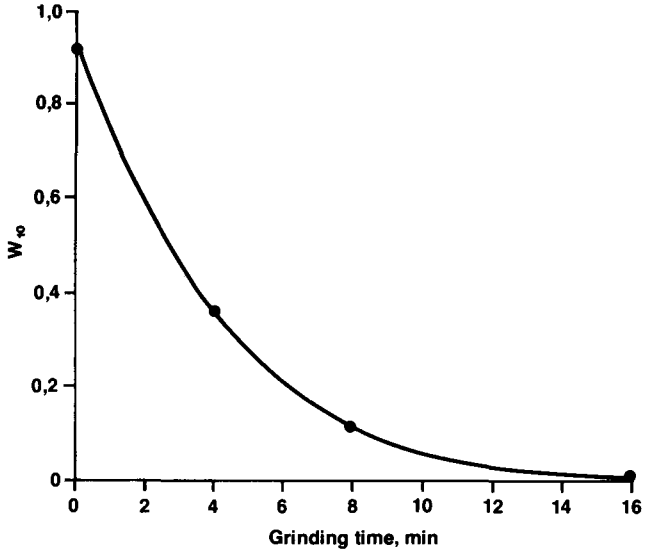

Fig. 14—W_{10}′ the fraction of material larger than size 10 (212 μm) versus grinding time (G/D = 1,2, R = −1, mill speed = 303 r/min, and ball size = 20 mm)

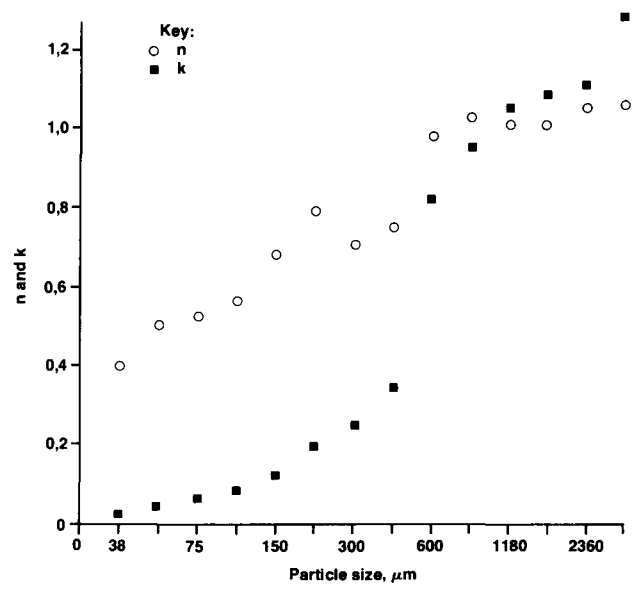

Fig. 15—Values for n and k as functions of particle size at 303 r/min, G/D = 1,2, and R = −1, 20 mm balls being used

A numerical technique that minimizes the value of the expression

$$\Sigma_j\left\{W_1(t_j) - \left[W_1(0)^{(1-n_1)} - k_1 t_j(1-n_1)\right]^{1/(1-n_1)}\right\}^2$$

for each size i by a non-linear regression routine will generally give more accurate results. The results for the example given above using the numerical method were as follows:

$$\frac{dW_{10}}{dt} = -0{,}21\ W_{10}{}^{0{,}81}.$$

Hence k_{10} = 0,21 and n_{10} = 0,81.

This procedure was carried out for each size to give k_1 and n_1 for i = 1 to 15, covering the size range 4700 to 38 μm. Fig. 15 shows the values for k and n as functions of size x. As an indication of the type of fit achieved, the sum of the squares of the differences between the actual values and those obtained from the model varied from $8{,}2 \times 10^{-9}$ (the best fit being at 850 μm) to $1{,}5 \times 10^{-3}$ (the worst fit being at 75 μm).

These errors were fairly typical, and Table III gives actual and predicted values of the size distribution for grinding times of 4 min, 8 min, and 16 min respectively.

If this technique is to be used as a model in the prediction of size distributions under varying operating conditions in a mill, some relationship must be found between the parameters n and k for the model, and the parameters N, R, G/D, and ball size for the mill. In practice, this has not been easy; the values for n and k do not seem to follow any simple functional form, and in some cases appear to be very scattered. However, work is continuing on the simplification of the functional forms of n and k without the introduction of unacceptable errors.

Conclusions

The particle mechanics within a centrifugal mill are not the same as those within a gravitational mill. The mill can be visualized as being in an acceleration field of varying magnitude and constant direction, or as

TABLE III

COMPARISON OF ACTUAL SIZE DISTRIBUTIONS WITH THOSE PREDICTED FROM THE CUMULATIVE BREAKAGE-RATE FUNCTION AT 303 r/min, G/D = 1,2, AND R = −1, 20 mm BALLS BEING USED

Size μm	n	k	t = 4,0 min		t = 8,0 min		t = 16,0 min		S.S. of errors
			Act. W_1	Pred. W_1	Act. W_1	Pred. W_1	Act. W_1	Pred. W_1	
38	0,419	0,048	0,789	0,808	0,656	0,641	0,353	0,356	0,61 E-3
53	0,518	0,060	0,741	0,763	0,588	0,569	0,265	0,269	0,85 E-3
75	0,545	0,080	0,659	0,688	0,477	0,452	0,131	0,139	0,15 E-2
106	0,583	0,098	0,597	0,627	0,397	0,369	0,061	0,071	0,18 E-2
150	0,700	0,135	0,503	0,526	0,280	0,254	0,009	0,027	0,15 E-2
212	0,812	0,212	0,365	0,365	0,118	0,117	0,001	0,004	0,88 E-5
300	0,724	0,261	0,255	0,255	0,035	0,035	0,001	0,001	0,36 E-6
425	0,768	0,356	0,146	0,146	0,006	0,006	0,001	0,000	0,25 E-6
600	1,000	0,838	0,064	0,050	0,002	0,002	0,000	0,000	0,21 E-3
850	1,052	0,975	0,024	0,023	0,001	0,001	0,000	0,000	0,82 E-8

S.S. = sum of squares
Act. = actual
Pred. = predicted

being in a rotating acceleration field of constant magnitude. In the first instance, the speed of rotation of the mill is taken relative to the rotating arm; in the second, it is taken relative to the earth.

For the representation of data obtained over several grinding times, the Schumann and Rosin–Rammler distributions provide reasonable fits over the finer particle sizes if the balls used are sufficiently large to break the largest particles. If the balls are too small to do this, an increase in the speed of the mill gives more force to the collisions, and the results obtained are in better agreement with the Schumann or Rosin–Rammler distributions.

After initial fast breakage, the rate of production of fines is linear up to about $Q(x, t) = 0{,}7$, bits constant rate of production being approximately proportional to the power consumption. The breakage of coarse particles shows some departure from first-order hehaviour. The departure from first-order breakage of coarse particles and zero-order production of fines during the initial stages of grinding is attributed to the presence of some soft or pre-fractured quartz that broke relatively quickly during the first few seconds of grinding.

The non-linear cumulative breakage rate function that was developed predicting behaviour in a mill has produced good results. It is hoped that further development will show the function to be a stable and reliable method of mill modelling.

Acknowledgements

This paper is published by permission of the Council for Mineral Technology (Mintek).

References

1. BRADLEY, A. A. Some principles of centrifugal milling. *3rd European Symposium on Size Reduction, Cannes, Oct. 1971.* Weinheim, Verlag Chemie, 1972. pp. 781 - 803.
2. BRADLEY, A. A., LLOYD, P. J. D., WHITE, D. A., and WILLOWS, P. W. High speed centrifugal milling and its potential in the mining industry. *S. Afr. Mech. Engr*, vol. 22, no. 4. 1972. pp. 129 - 134.
3. JOISEL, A. *Rev. Mater. Constr. Trav. Publ.*, no. 493. 1956. pp. 234 - 250.
4. AUSTIN, L. G., LUCKIE, P. T., and KLIMPEL, R. R. The design of grinding circuits. South African Institute of Mining and Metallurgy, Vacation School on Grinding — Theory and Practice, 8th to 12th August, 1977.
5. HERBST, J. A., and FUERSTENAU, D. W. The zero order production of fine sizes in comminution and its implications in simulation. *Trans. Soc. Min. Engrs AIME*, vol. 142. 1968. pp. 538 - 548

Automation

The fourth Symposium on Automation in Mining, Mineral and Metal Processing is to be held in Helsinki from 22nd to 25th August, 1983. The Symposium is sponsored by the International Federation of Automatic Control (IFAC) and is being organized by the Finnish Society of Automatic Control.

The Symposium will deal with the latest developments in control application, equipment, and theory in the mining, mineral, and metal-processing industries. The preceding symposia of this successful series were held in Sydney, Johannesburg, and Montreal. The language of the Symposium is English.

Papers are invited that describe and analyse new applications and developments in the following and related processes.

Mining

Prospecting; computer-aided mine design techniques; material handling; transportation; mining equipment and methods; environmental control; monitoring; remote control; equipment dispatching and production scheduling.

Mineral Processing

Crushing; grinding; classifying; flotation and other concentrating methods for metallic and non-metallic minerals; agglomeration; kilns operation; other beneficiation methods; energy minerals.

Extractive Metallurgy

Sintering; pyrometallurgy; blast furnaces; direct reduction; electrolysis.

Metal Processing

Steelmaking; non-ferrous metal production; reheat furnaces; rolling mills; continuous casting; annealing.

Papers on topics of instrumentation, control and systems engineering that are relevant to the above processes and industries are also invited.

Further information is available from Mr G. Sommer, Mintek, Private Bag X3015, Randburg (telephone: (011) 793-3511) or from IFAC 4th MMM Symposium 1983, Secretariat, P.O. Box 192, SF-00101 Helsinki 10, Finland (telephone: 358-0-6941466, telex 121845 ahaka sf).

The Trevithick Society

The Trevithick Society, named after Cornwall's greatest engineer, was founded for the study of the history of industry and technology in Cornwall.

It began life in 1935 as the Cornish Engines Preservation Society and, as a result of its efforts, five of these magnificent examples of Cornish engineering skill were rescued and put into the care of the National Trust. One is a giant, with a cylinder 90 inches in diameter.

The Society later combined with the Cornish Waterwheel Preservation Society and is one of the oldest Industrial Archaeological Societies in Britain, if not the world.

Today the Society is concerned with the study of the history of Industry and Technology in Cornwall and publishes an annual Journal and a quarterly Newsletter, plus other works concerning this subject.

Anyone interested in joining the Society should write to Mr T.M.P. Tarrant, Membership Secretary, 8 Crossfield Avenue, Cowes, Isle of Wight PO31 8HB, U.K.